Analysis of the Cure of Epoxy Based Layered Silicate Nanocomposites: Reaction Kinetics and Nanostructure Development

S. Montserrat,[1] F. Román,[1] J. M. Hutchinson,[1] L. Campos[2]

[1]*Departament de Màquines i Motors Tèrmics, ETSEIAT, Universitat Politècnica de Catalunya, 08222 Terrassa, Spain*
[2]*Departament d'Enginyeria Química, ETSEIB, Universitat Politècnica de Catalunya, 08208 Barcelona, Spain*

Received 17 April 2007; accepted 16 July 2007
DOI 10.1002/app.27297
Published online 18 January 2008 in Wiley InterScience (www.interscience.wiley.com).

ABSTRACT: The cure reaction kinetics of epoxy resin, with organically modified montmorillonite loadings of up to 20 wt % and with stoichiometric conditions, has been studied by differential scanning calorimetry with a view to understanding further the fabrication of epoxy-based polymer layered silicate nanocomposites. The kinetic analysis of isothermal and nonisothermal cure shows that the autocatalytic model is the more appropriate to describe the kinetics of these reactions, and it is observed that a dominant effect of the montmorillonite is to catalyze the curing reaction. However, it was not possible to model the reactions over the whole range of degrees of conversion, in particular for nonisothermal cure. This attributed to the complexity of the reactions, and especially to the occurrence of etherification by cationic homopolymerization catalyzed by the onium ion of the organically modified montmorillonite. The homopolymerization reaction results in an excess of diamine in the system, and hence in practice the reaction is off stoichiometric, which leads to a reduction in both the heat of cure and the glass transition temperature as the montmorillonite content increases. Small angle X-ray scattering of the cured nanocomposites shows that an exfoliated nanostructure is obtained in nonisothermal cure at slow heating rates, whereas for nonisothermal cure at faster heating rates, as well as for isothermal cure at 70°C and 100°C, a certain amount of exfoliation is accompanied by the growth of *d*-spacings of 1.4 nm and 1.8 nm for dynamic and isothermal cure, respectively, smaller than the *d*-spacings of the modified clay before intercalation of the resin. A similar nanostructure, consisting of extensive exfoliation accompanied by a strong scattering at distances less than the *d*-spacing of the modified clay, is also found for resin/clay mixtures, before the addition of any crosslinking agent, which have been preconditioned by storage for long times at room temperature. The development of these nanostructures is attributed to the presence of clay agglomerations in the original resin/clay mixtures and highlights the importance of the quality of the dispersion of the clay in the resin in respect of achieving a homogeneous exfoliated nanostructure in the cured nanocomposite. © 2008 Wiley Periodicals, Inc. J Appl Polym Sci 108: 923–938, 2008

Key words: nanocomposite; DSC; cure kinetics; montmorillonite; glass transition; epoxy; layered silicate

INTRODUCTION

Polymer layered silicate (PLS) nanocomposites are well known to offer potential advantages as high performance materials for a number of reasons. For example, they can provide a significant enhancement of mechanical properties, such as modulus and strength, in comparison with the unmodified polymer. Of particular importance, though, is the observation that, in contrast to conventional composite materials for which the reinforcement is on a macroscopic scale, the enhancement in mechanical properties in these PLS nanocomposites can be achieved at very low silicate loadings. This has obvious benefits in respect of the density of the nanocomposite and is therefore of particular interest to the aerospace industry. There are some excellent recent reviews in which these aspects of nanocomposite performance are summarized, for PLS nanocomposites in general[1,2] as well as for epoxy-based PLS nanocomposites in particular.[3]

Nevertheless, it is also clear that these potential improvements in properties are not always realized in the nanocomposites. The reason for this is that such property enhancement requires a certain nanostructure to be achieved during the fabrication process, in particular a structure in which the silicate layers are exfoliated and distributed homogeneously throughout the polymer matrix. The mechanisms by which exfoliation takes place depend on the layered nanocomposite system, that is to say whether the fabrication process is by melt intercalation of the resin or by in situ polymerization. In PLS nanocomposites based on epoxy resin it is the latter process which is relevant, and is the one that is investigated in the present article.

Correspondence to: S. Montserrat (montserrat@mmt.upc.edu).

Contract grant sponsor: CICYT Project; contract grant number: MAT2004-04165-C02-01.

©2008 Wiley Periodicals, Inc.
WILEY InterScience® DISCOVER SOMETHING GREAT

However, although exfoliation is frequently reported to have been achieved, on the evidence of X-ray data or transmission electron microscopy (TEM), in a variety of resin and hardener systems, there are also many reports of either incomplete exfoliation or no exfoliation at all under some circumstances. Furthermore, while it is often suggested that exfoliation depends on the balance between the intra-gallery and extra-gallery polymerization rates [e.g., Refs. 4 and 5], there are other factors, such as preconditioning the resin/clay mixture before adding the hardener and curing the nanocomposite,[6] which appear to play an important part. In addition, this suggestion about the balance of polymerization rates still leaves unspecified the actual molecular mechanisms responsible for the exfoliation while also leaving unanswered some basic questions: for example, what is the role of stoichiometry in the exfoliation process and what evidence is there that there is a stoichiometric ratio of resin and hardener in the two regions, intra- and extra-gallery? Until such questions are answered and the mechanisms of exfoliation established more clearly, it will not be possible to benefit fully from the potential advantages of these nanocomposites for any given resin and hardener system. One possible route toward achieving such an end is to investigate the kinetics of the curing reaction for the resin/clay/hardener system.

There has been a significant amount of effort devoted to such studies over the past 5 years or so.[5,7–16] One immediate observation that can be made from these investigations is that, even when the epoxy resin and hardener system is the same, for example diglycidyl ether of bisphenol-A (DGEBA) epoxy cured with an amine, and the nanoclay is an organically modified montmorillonite (MMT), the kinetics of the curing reaction can vary significantly and can display a number of different features depending upon the conditions of the cure process. As a consequence, the nanocomposite which results may be fully or partially exfoliated, or not exfoliated at all, which has a corresponding effect on the properties of the cured nanocomposite. However, it is not easy to use these results to define the optimum conditions for any given nanocomposite system to obtain homogeneous exfoliation of the clay, because of the large number of experimental variables that can have an influence. For example, the cure may be either isothermal or nonisothermal, including a range of isothermal cure temperatures and of nonisothermal cure rates, the organically modified MMT content can vary considerably, and there are various possibilities for the preparation procedure for the resin/clay mixture, which can involve lengthy periods of time at temperatures sufficiently far above ambient such that some homopolymerization can take place before the curing schedule.

As an illustration of this difficulty, consider the effect of clay content on the glass transition temperature, T_g, of the cured nanocomposite, for which there are occasionally apparently conflicting results presented. For example, in the same DGEBA plus amine plus organically modified MMT system Ton-That et al.[12] report that the T_g of the cured nanocomposite with 2 wt % clay is lower, by about 4°C, than that for the epoxy/diamine without clay, whereas Ivankovic et al.[16] find a decrease of 2°C for the 5 wt % nanocomposite but an increase of 6°C for a clay content of 10 wt %. Direct comparison of these results is not helpful, though, as the former cure schedule was dynamic at rates between 2.5 and 20 K/min whereas the latter was isothermal at cure temperatures between 91°C and 101°C, always higher than the T_g of the cured nanocomposite.

In addition to these difficulties, Benson Tolle and Anderson recently reported that a further aspect of the preparation procedure for the resin/clay mixture can have a very significant effect on the exfoliation process.[6] These authors found that storage of the mixture at room temperature for long periods of time (several weeks) before adding the curing agent and curing the nanocomposite, a process which they referred to as preconditioning, dramatically enhanced the exfoliation rate as observed by X-ray diffraction, and they attributed this to ''some epoxy reaction.'' If this is indeed the case, then storage of the resin/clay mixture before determining the curing reaction kinetics would have a significant effect since some reaction of the epoxy groups would already have occurred. In a more recent study,[17] we concluded that it was homopolymerization of the epoxy resin, catalyzed by the onium ion of the modified MMT, that was occurring, even at room temperature, and hence that any reaction kinetics studies must be undertaken with this effect in mind.

The objectives of the present article are therefore twofold: to investigate the isothermal and nonisothermal cure reaction kinetics of a nanocomposite system, consisting of an epoxy resin plus modified MMT plus hardener, as a function of the nanoclay content; and to examine in some detail the effect of the cure schedule on the nanostructure of the cured samples.

EXPERIMENTAL

Materials

A commercial organically modified MMT, supplied by Nanocor (Arlington Heights, IL), was used in this study. This organoclay has the trade name Nanomer I.30E and is an octadecylammonium-treated MMT with a density of approximately 1.7 g/cm^3 according to the manufacturer's literature.

The epoxy resin used (Epon 828, Shell Chemicals [Resolution Performance Products, Houston, TX]) is based on DGEBA and has a density of 1.16 g/cm^3 and a viscosity of 110–150 Poise (11,000–15,000 mPa s) at 25°C. The epoxide equivalent (ee) weight is in the range 185–192 g/ee. The crosslinking agent used was a diamine, Jeffamine D-230 from Huntsman Corp. (Salt Lake City, UT).

Preparation of resin/clay mixtures

The resin and clay were mixed at room temperature using a mechanical stirrer, followed by degassing in a vacuum oven. Four weight percentages of clay in the resin/clay mixture were used, namely 2 wt %, 5 wt %, 10 wt %, and 20 wt %, and the samples were cured using a stoichiometric amount of the curing agent. The nanocomposites with 2, 5, 10, and 20 wt % clay are denoted, respectively, as NEPAJ2, NEPAJ5, NEPAJ10, and NEPAJ20, and are compared with the resin/hardener system without any clay, denoted as EPJ. The detailed compositions for all these samples are listed in Table I.

TABLE I
Proportions of Epoxy, Diamine, and Montmorillonite in Nanocomposite Samples

Sample	% MMT in resin/clay	Sample composition (wt %)		
		Epoxy	Jeffamine	MMT
EPJ	0	76.0	24.0	0
NEPAJ2	2	74.9	23.6	1.5
NEPAJ5	5	73.1	23.1	3.8
NEPAJ10	10	70.1	22.1	7.8
NEPAJ20	20	63.8	20.2	16.0

Optical microscopy

The dispersion of the clay in the resin was observed using a Leica polarising transmission optical microscope.

Small angle X-ray scattering

The intercalation of the resin in the clay galleries was investigated by small angle X-ray scattering (SAXS). X-ray diagrams were recorded on film under vacuum at room temperature, and molybdenum disulphide (d = 0.6147 nm) was used for calibration. A modified Statton camera (W. R. Warhus, Wilmington, DE) using a pinhole collimator with Ni-filtered copper radiation of wavelength 0.1542 nm was used for these experiments. All samples were studied within sealed quartz capillaries.

Differential scanning calorimetry

The curing reactions of the resin/clay/hardener mixtures were studied using a Mettler-Toledo DSC 821^e calorimeter equipped with a sample robot and Haake EK90/MT intracooler. Data evaluation was performed with the STAR^e software. The differential scanning calorimetry (DSC) was calibrated for both heat flow and temperature using indium.

In view of the fact (as will be seen later) that the crosslinking reaction begins almost immediately after the addition of the hardener to the resin/clay mixture, an experimental protocol was adopted to ensure that a minimum amount of the heat of reaction is lost in the time between sample preparation and insertion into the calorimeter. For isothermal and nonisothermal cure schedules, this protocol involved preheating the DSC furnace to the isothermal temperature or to the starting temperature for the nonisothermal scan, respectively, before the sample is inserted by the robot. For all curing experiments, the hardener was added in the required stoichiometric proportion to a small amount of the resin/clay mixture in a watch-glass and was stirred sufficiently by hand to ensure a homogeneous mixture. From this mixture, a sample of about 7 mg to 8 mg of resin/clay/hardener was weighed into an aluminum crucible, the lid (with a pierced hole) was sealed onto the crucible, and the sample was then immediately inserted into the DSC furnace and the curing experiment was immediately started. The calorimeter requires a ''settling time'' of between 5 and 10 s to establish equilibrium, and the typical time from mixture of the hardener to starting the experimental measurements was about 1 min. Each mixture in the watch-glass was used for only a single curing experiment; in other words, every curing experiment involved a fresh mixture of the hardener with the preprepared batch of resin/clay mixture.

All DSC curing experiments were performed with a dry nitrogen gas flow of 50 mL/min. Isothermal experiments were made at cure temperatures between 60°C and 110°C, for cure times long enough for the heat flow to return to a horizontal baseline. These isothermal cures were followed immediately by a second (nonisothermal) scan at 10 K/min from −10°C to 280°C to determine the glass transition temperature, T_g, of the material after the isothermal cure and to measure any residual heat of cure, and then by a third scan, at 10 K/min over a narrower temperature range, to determine the T_g of the fully cured material. Between each scan the sample was cooled in the DSC at a controlled rate of −20 K/min. Nonisothermal scans were made at rates between 2.5 K/min and 20 K/min over a temperature range from 25°C to 280°C, and were followed by a second scan at 10 K/min to determine the T_g.

KINETIC ANALYSIS

The fundamental kinetic equation describing the rate of the chemical reaction taking place during the curing process can be written in the form:

$$d\alpha/dt = k(T)f(\alpha) \quad (1)$$

where α is the degree of cure at time t. The influence of temperature (T) on the reaction is introduced through the rate constant $k(T)$, which is usually assumed to have an Arrhenius temperature dependence:

$$k(T) = A\exp(-E/RT) \quad (2)$$

in which A is a pre-exponential factor and E is the activation energy for the process. The function $f(\alpha)$ in eq. (1) represents the mathematical expression of the kinetic model, and can take several different forms. In the DSC experiments, the heat flow ϕ that is measured and which results from the curing reaction is assumed to be proportional to the rate of cure:

$$\phi = (d\alpha/dt)\ \Delta H_{\text{tot}} \quad (3)$$

where ΔH_{tot} is the total heat of cure of the reaction, which in this work has been determined from the area under a nonisothermal DSC curing scan or from an isothermal curing experiment taking into account any residual heat evolved in a subsequent nonisothermal scan.

Equations (1)–(3), together with a suitably defined $f(\alpha)$, are usually applied to describe the time and temperature dependence of the degree of cure in both isothermal and nonisothermal DSC cure experiments, so that, in principle, the various parameters of the kinetic models can be evaluated by an appropriate fitting procedure. However, it has been shown[18] that there is a strong correlation between the activation energy E and the pre-exponential factor A, as a consequence of which the usual multiple regression algorithms for the evaluation of the kinetic parameters are inadequate unless at least one of these parameters can be determined independently.

One approach is first to evaluate the activation energy by a direct method, and subsequently to determine $\ln(A)$ and the kinetic parameters of the function $f(\alpha)$. In this work, the apparent activation energy is found by the Friedman isoconversional method,[19] which leads to the determination of the activation energy as a function of the degree of conversion, thus allowing for the possibility of checking for the invariance of the activation energy during the cure. Under isoconversional conditions (α = constant), combining eqs. (1)–(3) gives:

$$\ln(\phi)_\alpha = \ln\,[Af(\alpha)] + \ln\,[\Delta H_{\text{tot}}] - E_\alpha/RT \quad (4)$$

Assuming that the function of the kinetic model, $f(\alpha)$, is not dependent on the temperature or the heating rate, the activation energy E_α for any degree of conversion α can be evaluated from the slope of a plot of the logarithm of the heat flow corresponding to that degree of conversion, $\ln(\phi)_a$, versus the reciprocal temperature. This method is applicable to both isothermal and nonisothermal cure experiments. The activation energy E_α may typically be subject to deviations of up to 10% as a result of experimental uncertainties, but if a significantly greater variation is observed this could imply that the reaction is more complex, involving a function $f(\alpha)$ which depends either on the temperature or on the heating rate.[20]

An alternative method for evaluating the activation energy is to use an approximation to the integral of the fundamental kinetic equation. This is the basis of the Kissinger[21] and Ozawa[22] methods, which gives a single ''overall'' activation energy for the complete cure process from the dependence on heating rate, β, of the temperature, T_p, at which the peak heat flow occurs in nonisothermal cure. In particular, for the Kissinger method this requires a linear least squares fit to a plot of $\log(\beta/T_p^2)$ versus $1/T_p$.

Once the activation energy has been determined, the other parameters are obtained from the DSC data by following the procedure devised by Málek.[18] This procedure consists of the evaluation of two functions, $y(\alpha)$ and $z(\alpha)$, applicable to both isothermal and nonisothermal experiments, and is used to distinguish between some specific kinetic models. These functions are defined as follows:[23]

$$y(\alpha) = \phi = \Delta H_{\text{tot}}\ kf(\alpha) \quad (5)$$

$$z(\alpha) = \phi t = \Delta H_{\text{tot}}\, f(\alpha)\, g(\alpha) \quad (6)$$

for isothermal experiments, or

$$y(\alpha) = \phi\exp(x) = \Delta H_{\text{tot}}\ Af(\alpha) \quad (5a)$$

$$z(\alpha) = \phi T^2 = Cf(\alpha)\, g(\alpha) \quad (6a)$$

for nonisothermal experiments, where $x = E/RT$ is a dimensionless quantity, $C = \Delta H_{\text{tot}}\ \beta E/RT$, and $g(\alpha) = \int_0^\alpha d\alpha/f(\alpha)$.

The functions $y(\alpha)$ and $z(\alpha)$ are invariant with respect to the temperature or the heating rate and are sensitive to small changes in the kinetic model $f(\alpha)$. In practice, both $y(\alpha)$ and $z(\alpha)$ are normalized in the interval $<0, 1>$ for convenience. The function $y(\alpha)$ is directly proportional to $f(\alpha)$ and the shape of the $y(\alpha)$ function plotted against α provides a direct means for identifying the most appropriate kinetic model.[23,24] For example, if the maximum in $y(\alpha)$ occurs at $\alpha_M = 0$, then the appropriate model is the reaction order model [$f(\alpha) = (1 - \alpha)^n$], whereas if the maximum occurs for $0 < \alpha_M < \alpha_P$, where α_P is

the value of α at the maximum in the heat flow curve, then it is the autocatalytic model [$f(\alpha) = \alpha^m (1 - \alpha)^n$]. As will be seen later, it is found in our curing experiments that the autocatalytic model is the more appropriate, and thus we present the further analysis relevant only to this kinetic model.

With the value of the activation energy having been determined independently, as described earlier, and the autocatalytic kinetic model having been selected, we can proceed to the evaluation of the other kinetic parameters. It can be shown[23] that the value of α at which the function $y(\alpha)$ passes through a maximum, α_M, can be used to evaluate the ratio $p = m/n$ of the two kinetic exponents of the autocatalytic model according to the equation:

$$p = \alpha_M/(1 - \alpha_M) \tag{7}$$

Equations (1)–(3) can be combined with the function $f(\alpha)$ of the kinetic model, which in the case of the autocatalytic model gives:

$$\phi\, e^x = A\, \Delta H_{tot}\, d^m (1 - \alpha)^n \tag{8}$$

which can be rewritten in logarithmic form as:

$$\ln [\phi\, e^x] = \ln [A\, \Delta H_{tot}] + n \ln [\alpha^{m/n}(1 - \alpha)] \tag{9}$$

Hence, a plot of $\ln [\phi\, e^x]$ versus $\ln [\alpha^{m/n} (1 - \alpha)]$ should yield a straight line with a slope equal to the value of the kinetic exponent n, while the other kinetic exponent can then be evaluated from the definition of p. Finally, the pre-exponential factor A can be found from the intercept, $\ln [A\, \Delta H_{tot}]$.

RESULTS

Intercalation and dispersion

The effect of mixing the resin and clay in the manner described in the Experimental section earlier has been discussed earlier in respect of the dispersion of the clay in the resin and the intercalation of the resin into the clay galleries.[17] We note that polarizing optical microscopy shows that the simple mechanical mixing procedure adopted here does not give as good a dispersion of the clay as does the mixing process using a solvent, in that some agglomerations of clay particles remain, with dimensions occasionally as large as 100 μm. Nevertheless, whether simple mixing or solvent mixing is used, the SAXS results show that the resin intercalates in the same way, with the *d*-spacing increasing from 2.09 nm for the modified clay alone, similar to other values reported in the literature[7,25–31] for the same commercial product, to values in the range 3.5 to 3.9 nm after mixing with the resin. No systematic dependence of the *d*-spacing on clay content was observed. The *d*-spacings for the intercalated clays are close to the theoretical limit of 3.74 nm calculated for the vertically oriented octadecyl anion.[4] We conclude from these results that the resin is well intercalated in the clay in our resin/clay mixtures. A typical SAXS diffraction pattern for a mechanically mixed sample containing 10 wt % clay is shown in Figure 1, where the intense inner ring at a (001) basal spacing of 3.75 nm ($2\theta = 2.35^\circ$) is followed by a weak reflection at half this spacing, and an outer ring at about 0.45 nm, corresponding to reflections from the (110) and (020) crystallographic planes of the clay layers.

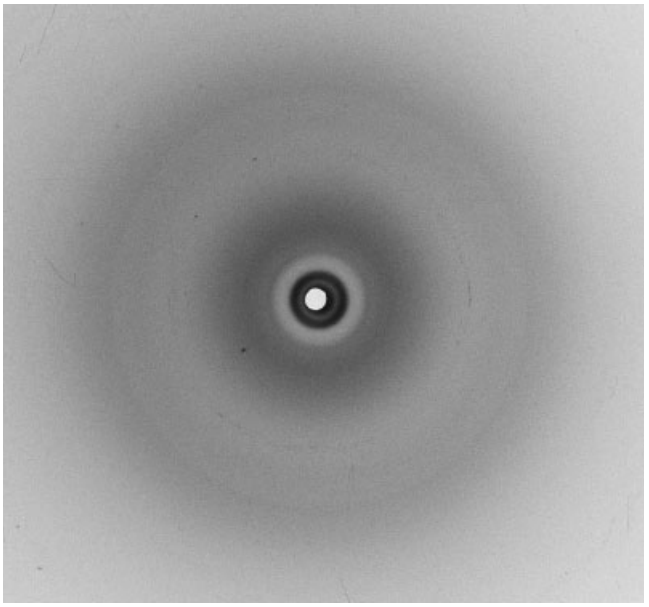

Figure 1 SAXS pattern for a sample of resin with 10 wt % MMT mixed by mechanical stirring for 20 h at 75°C.

In view of the fact that the resin intercalates into the clay galleries in essentially the same way for all the resin/clay mixtures, the less than ideal dispersion of the clay in the resin for these simple mixtures was not originally expected to have an influence on the curing kinetics. In contrast, it would be expected to have a significant effect on the mechanical properties, and particularly on the limiting properties such as strength and strain at failure, for which the occurrence of stress concentrations initiated by clay particle agglomerations would play an important role. Nevertheless, as will be shown later, it transpired that there were certain circumstances in which the nanostructure of the cured nanocomposite, as revealed by SAXS, displayed features which could be interpreted in terms of a poor dispersion of the clay. Accordingly, in future work we intend to compare the cure kinetics of solvent-prepared mixtures, for which a significantly better dispersion of the clay is observed, with the results obtained here.

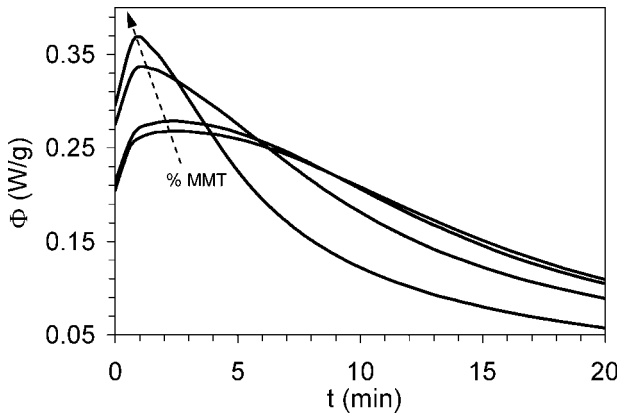

Figure 2 DSC scans for the isothermal cure at 90°C of the epoxy and diamine without clay (EPJ) and for the nanocomposites with 2 wt % (NEPAJ2), 5 wt % (NEPAJ5), and 20 wt % (NEPAJ20) montmorillonite. The arrow indicates the direction of increasing clay content. The specific heat flow (Φ) is referred to the total mass of the sample, including the mass of the clay. Note that, for clarity, only a part of the complete isotherm at each temperature is shown here.

DSC data

A typical result for the heat flow as a function of time during an isothermal curing experiment is shown in Figure 2 for an isothermal temperature of 90°C. It can be seen that the addition of the montmorillonite generally causes an advance in the reaction such that the peak of the heat flow tends to increase in magnitude and to occur at shorter times as the MMT content increases. It is quite clear, therefore, that the addition of the modified MMT has a significant catalytic effect on the cure reaction.

Second and third scans were made following each of the isothermal cures for all the samples, and the results are gathered in Table II in respect of the glass transition temperatures of the partially cured sample after the second scan ($T_{g,\text{part}}$) and of the final nanocomposite after the third scan ($T_{g,fr\text{iso}}$), the partial heat of reaction during the isotherm and the residual heat of cure during the second scan (ΔH_{part} and ΔH_{res}, respectively) as well as the total heat of reaction (ΔH_{tot}), which is the sum of the partial and residual heats. Also included in the Table are the cure times (t_c) at each temperature (T_c) and the times (t_p) for which the peak heat flow occurs. To compare the different samples, the total heat of reaction is given with reference to both the total sample mass and per epoxy equivalent.

For the nonisothermal cure experiments, Figure 3 shows a typical set of curves for four of the systems studied at a heating rate of 2.5 K/min. Similar to the case for the isothermal experiments in Figure 2, the addition of MMT results in an advance of the reaction, such that the initial rise in the heat flow as well as the peak heat flow both occur at lower temperatures as the MMT content increases. The heat of reaction and the temperature for maximum heat flow (T_p) are found from such curves,

TABLE II
Isothermal Cure Data for the Nanocomposite Samples

T_c (°C)	t_c (min)	t_p (min)	$T_{g,\text{part}}$ (°C)	$T_{g,f,\text{iso}}$ (°C)	ΔH_{part} (J/g)	ΔH_{res} (J/g)	ΔH_{tot} (J/g)	ΔH_{tot} (kJ/ee)
EPJ								
70	360	6.7	73.6	86.6	386.0	14.1	400.1	100.0
90	225	2.5	84.9	88.3	391.5	12.3	403.9	101.0
100	180	1.0	84.8	86.6	380.0	4.5	384.6	96.1
110	150	0.6	84.6	85.3	368.2	7.5	375.7	93.9
NEPAJ2								
70	360	4.0	73.1	82.7	389.3	10.1	399.4	101.4
80	300	2.8	78.3	82.9	365.7	6.9	372.6	94.6
90	225	2.2	81.2	84.2	388.3	5.5	393.8	100.0
100	180	0.6	80.5	82.3	350.6	3.3	353.9	89.9
NEPAJ5								
70	360	7.8	71.5	80.3	393.3	10.4	403.7	105.0
80	300	2.2	78.0	83.3	365.0	9.7	374.7	97.4
90	225	1.2	78.5	82.0	373.8	6.1	379.9	98.8
100	180	0.6	80.2	82.2	374.1	6.0	380.0	98.8
NEPAJ10								
70	360	2.3	71.4	81.3	332.2	18.7	350.9	95.1
80	300	3.7	77.1	82.9	354.3	10.9	365.3	99.0
90	225	1.0	77.1	82.5	333.6	10.6	344.3	93.3
100	180	0.7	73.0	77.4	332.3	10.9	343.2	93.0
NEPAJ20								
60	540	5.0	51.5	62.8	284.6	22.1	306.7	91.3
70	360	2.7	65.8	76.0	329.6	14.3	343.9	102.4
80	300	1.2	71.5	77.1	311.4	9.4	320.8	95.5
90	225	0.9	68.8	75.1	278.4	8.2	286.7	85.4
100	180	0.9	70.2	75.5	274.9	5.2	280.1	83.4

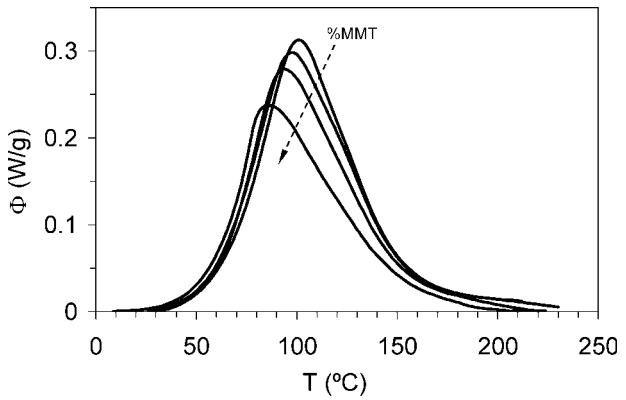

Figure 3 DSC scans for nonisothermal cure at 2.5 K/min of four different systems (EPJ, NEPAJ5, NEPAJ10, and NEPAJ20). The arrow indicates the direction of increasing clay content. The specific heat flow (Φ) is obtained by reference to the total sample mass, including the clay.

while the second scan gives the final glass transition temperature of the nonisothermally cured nanocomposite ($T_{g,f,\text{noniso}}$) and verifies that the heat of reaction is indeed the total heat in that there is no significant residual curing reaction. The data obtained in this way for all the nanocomposite systems and for all heating rates for the nonisothermal cure are summarized in Table III.

TABLE III
Nonisothermal Cure Data for the Nanocomposite Samples

β (K/min)	ΔH_{tot} (J/g)	ΔH_{tot} (kJ/ee)	T_p (°C)	$T_{g,f,\text{noniso}}$ (°C)
EPJ				
2.5	431.8	107.9	101.2	85.9
5	430.8	107.7	114.6	85.5
10	415.6	103.9	127.8	86.1
15	418.8	104.7	137.3	85.9
20	419.4	104.8	144.5	85.0
NEPAJ2				
2.5	444.3	112.9	99.5	83.1
5	437.6	111.2	112.7	82.6
10	397.8	101.1	125.2	77.7
15	394.2	100.1	134.2	82.3
20	398.4	101.2	141.9	86.3
NEPAJ5				
2.5	439.8	114.5	97.9	82.3
5	382.2	99.5	110.5	80.9
10	387.9	101.0	123.9	80.4
15	366.8	95.5	131.2	82.3
20	377.3	98.2	137.3	82.3
NEPAJ10				
2.5	384.4	104.2	93.7	79.4
5	362.3	98.2	109.3	81.0
10	333.0	90.3	122.3	80.9
15	355.0	96.2	130.2	81.0
20	360.9	97.1	136.4	80.0
NEPAJ20				
2.5	348.8	103.9	86.2	75.4
5	342.6	102.0	104.5	74.0
10	322.8	96.1	119.1	74.4
15	310.7	92.5	127.2	73.1
20	328.2	97.7	132.9	74.3

Activation energy and kinetic analysis

The isoconversional method for the evaluation of the activation energy from the isothermal cure data at the different temperatures involves plotting, as a function of the reciprocal of the isothermal cure temperature, the logarithm of the heat flow corresponding to selected values of α, usually taken in intervals of 0.1 from 0.1 to 0.9. As an illustration, the results obtained for the sample NEPAJ5 are shown in Figure 4, where it can be seen that there is a good linear relationship, as required by eq. (4), and from a least squares fit to the data the isoconversional activation energy can be determined for each value of α. Similar results are obtained for the other samples listed in Table I, and the values of activation energy thus found for each sample and for each value of α are plotted in Figure 5. In general, the activation energy decreases somewhat with increasing α, for reasons to be discussed later. The notable exception is NEPAJ20, for which the increase in E_α results from vitrification at the lower isothermal temperatures. For the purposes of the kinetic analysis, which requires a unique value for the activation energy, we take the average from Figure 5 over the whole range of α.

The isoconversional activation energy can be determined in an analogous way from nonisothermal data, and is plotted as a function of α in Figure 6 for the five systems studied here. Again, similar to the situation for the isothermal isoconversional activation energy, but rather more pronounced than in that case, there is a certain variation in the activation energy, which needs to be considered to apply a

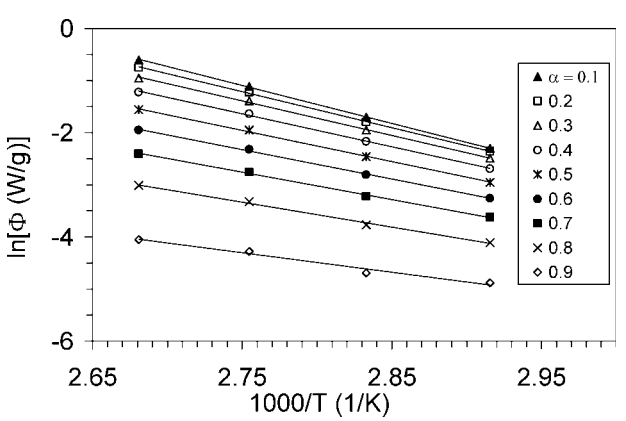

Figure 4 Logarithm of the heat flow corresponding to various degrees of cure, α, as indicated, as a function of reciprocal temperature for NEPAJ5 cured isothermally at 70, 80, 90, and 100°C. The full lines represent least squares fits to each set of data for constant α.

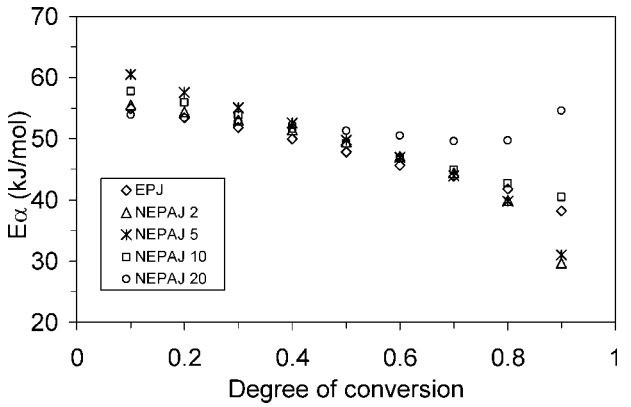

Figure 5 Activation energy as a function of degree of cure for the isothermal cure experiments.

unique value of activation energy in the kinetic analysis. In particular, there is often a significant deviation for the extreme values of α of 0.1 and 0.9. Hence, for these purposes we make use of the average value over the slightly more limited range of α from 0.2 to 0.8, inclusive, for all the nanocomposite samples, additionally incorporating into the average the values of E at α = 0.1 for NEPAJ10 and at α = 0.9 for NEPAJ20, for which the deviations are only small.

The overall activation energy for each nanocomposite can also be determined by the Kissinger method. The results obtained for the activation energy by the isoconversional method for both isothermal and nonisothermal experiments and by the Kissinger method, for all the samples, are compiled in Table IV for comparison. The average isoconversional activation energies are the values used in the kinetic analysis that follows, given separately for the isothermal and nonisothermal cure experiments.

Since the procedures for the kinetic analysis of isothermal and nonisothermal data are very similar, we illustrate here only the latter. The $y(\alpha)$and $z(\alpha)$ functions are calculated according to eqs. (5a) and (6a), respectively, and are normalized in the interval <0, 1>. Figure 7 shows their variation for samples EPJ [Fig. 7(a)] and NEPAJ10 [Fig. 7(b)], with the data for all five heating rates superposed. As anticipated by the theoretical analysis, these two functions are to a good approximation independent of the heating rate over a wide range of α and more so for the sample (EPJ) without MMT (the more marked deviations for the sample NEPAJ10 are discussed in Section on Kinetic Analysis later). The maximum in $y(\alpha)$ occurs at a value of α greater than zero, and hence the autocatalytic model is the more appropriate, and the value of p is found from this value of α. The parameter n

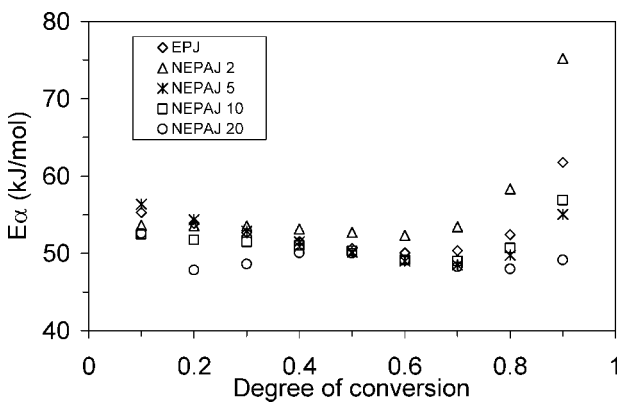

Figure 6 Activation energy as a function of degree of cure for the nonisothermal cure experiments.

TABLE IV
Summary of Activation Energy Values: Average Isoconversional Values from Isothermal, *E* (av. iso), and Nonisothermal Cure, *E* (av. noniso), and Overall Value from Kissinger Analysis, *E* (Kissinger)

Sample	*E* (av. iso)	*E* (av. noniso)	*E* (Kissinger)
EPJ	47.5	51.6	56.2
NEPAJ2	47.2	53.9	57.4
NEPAJ5	48.6	50.9	60.4
NEPAJ10	49.3	50.7	55.0
NEPAJ20	52.0	48.8	47.6

All values are in kJ/mol.

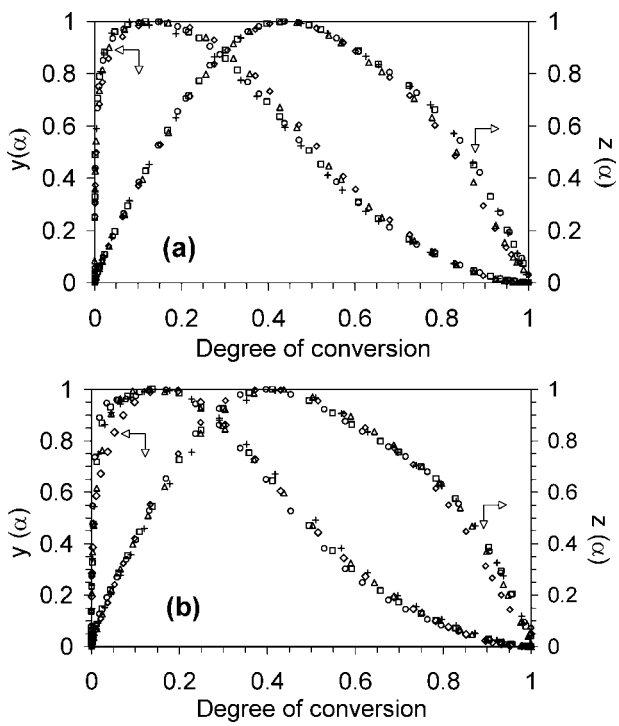

Figure 7 $y(\alpha)$ and $z(\alpha)$, normalized in the interval <0, 1>, as a function of α during nonisothermal cure at 2.5 (◇), 5 (△), 10 (+), 15 (□), and 20 K/min (○) for (a) EPJ and (b) NEPAJ10.

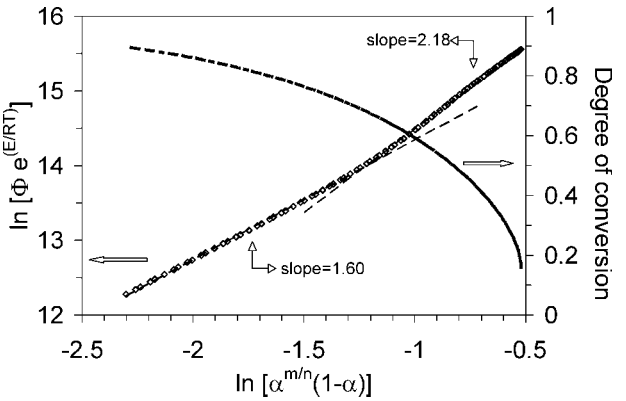

Figure 8 Plot of ln [ϕe^x] versus ln [$\alpha^{m/n}$ (1 − α)] for nonisothermal cure of NEPAJ10 at 10 K/min. The points refer to the left-hand axis, while the crosses refer to the degree of cure indicated on the right-hand axis.

is evaluated from the double logarithmic plot of [ϕ e^x] versus [$\alpha^{m/n}$ (1 − α)], a typical example being shown in Figure 8 for the sample NEPAJ10. It is evident that this plot represents two separate straight lines rather than the single straight line which is predicted theoretically, the change in slope between the two linear regions being even more marked for nonisothermal cure than for isothermal cure. For the purposes of evaluating the exponent n, we take here the slope corresponding to the initial part of the reaction, as shown by the dashed line with slope 2.18 that is fit to this part of the data (it should be noted that, in the graphical representation of Figure 8, the reaction proceeds from right to left). The other exponent m is then evaluated as the product of n and p, and the pre-exponential factor A is found from the intercept. Summaries of the kinetic parameters for both isothermal and nonisothermal cure are given in Tables V and VI.

TABLE V
Kinetic Parameters Evaluated by Malek's Method from Isothermal Data

T_c (°C)	α_M	m	n	ln[A] (s^{-1})
EPJ				
70	0.088	0.12	1.29	8.79
90	0.086	0.15	1.57	8.97
100	0.078	0.14	1.62	9.02
110	0.085	0.15	1.57	9.14
NEPAJ2				
70	0.069	0.11	1.46	8.70
80	0.070	0.12	1.54	8.78
90	0.092	0.15	1.49	8.89
100	0.050	0.10	1.84	9.04
NEPAJ5				
70	0.094	0.15	1.47	9.21
80	0.055	0.08	1.47	9.23
90	0.078	0.15	1.83	9.58
100	0.052	0.10	1.86	9.53
NEPAJ10				
70	0.042	0.06	1.43	9.43
80	0.109	0.20	1.65	9.76
90	0.064	0.12	1.70	9.80
100	0.053	0.10	1.75	9.77
NEPAJ20				
60	0.067	0.15	2.07	10.94
70	0.052	0.10	1.75	10.79
80	0.070	0.14	1.89	11.09
90	0.054	0.11	2.01	10.98
100	0.130	0.40	2.67	11.65

DISCUSSION

Activation energy

The cure process involves several possible reactions,[32,33] as illustrated schematically in Figure 9: (i) the reaction of the epoxide groups with the primary amine; (ii) the reaction of the epoxide groups with the secondary amine; (iii) etherification via the secondary amine, being catalyzed by the tertiary amine;[34] and (iv) etherification via homopolymerization, being a cationic polymerization process catalyzed by the onium ion of the organically modified MMT.[35,36] The last of these reactions was identified in our earlier work[17] as being important, in particular with respect to ''preconditioning'' of resin/clay mixtures prior to the addition of the crosslinking

TABLE VI
Kinetic Parameters Evaluated by Malek's Method from Nonisothermal Data

β (K/min)	α_M	m	n	ln[A] (s^{-1})
EPJ				
2.5	0.15	0.38	2.10	10.78
5	0.15	0.38	2.13	10.84
10	0.09	0.19	1.83	10.55
15	0.13	0.29	1.90	10.64
20	0.13	0.29	1.93	10.65
NEPAJ2				
2.5	0.10	0.22	2.07	11.30
5	0.09	0.21	2.12	11.32
10	0.07	0.17	2.07	11.35
15	0.11	0.27	2.25	11.51
20	0.09	0.22	2.17	11.47
NEPAJ5				
2.5	0.14	0.35	2.12	10.60
5	0.13	0.32	2.12	10.64
10	0.13	0.34	2.17	10.80
15	0.09	0.23	2.17	10.65
20	0.11	0.29	2.27	10.79
NEPAJ10				
2.5	0.17	0.49	2.21	10.75
5	0.13	0.30	2.02	10.59
10	0.16	0.41	2.18	10.88
15	0.16	0.47	2.46	11.05
20	0.15	0.44	2.51	10.99
NEPAJ20				
2.5	0.21	0.73	2.67	10.88
5	0.14	0.37	2.19	10.16
10	0.10	0.23	2.11	10.11
15	0.08	0.20	2.17	10.16
20	0.12	0.29	2.14	10.38

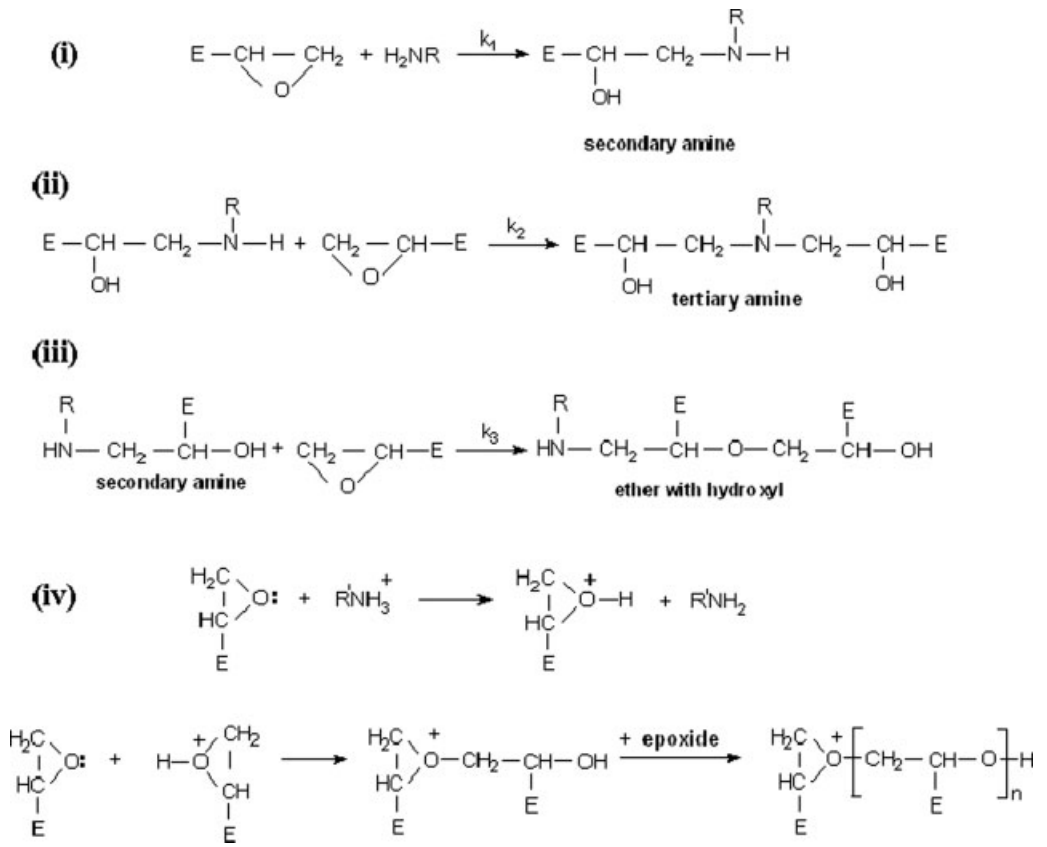

Figure 9 Schematic illustration of the various reactions that may occur during the crosslinking of epoxy nanocomposite samples.

agent, which has been reported to have a significant influence on the exfoliation process.[6] Nevertheless, in spite of the complexity of the reaction mechanisms, the activation energy, shown in Figures 5 and 6 for isothermal and nonisothermal cure, respectively, varies relatively little over a major part of the reaction, from $\alpha = 0.2$ to $\alpha = 0.8$ approximately. The average values of E used for the kinetic analysis (Table IV) fall within the ranges 47.2 to 52.0 kJ/mol for isothermal cure and 48.8 to 53.9 kJ/mol for nonisothermal cure, for the five different nanocomposite systems. When compared with the values of E obtained by the Kissinger method, given earlier, it can be seen that, with the exception of NEPAJ20, the isoconversional values are about 10% lower.

The slight tendency in Figures 5 and 6 for E_α to decrease with increasing degree of cure, at least until a conversion of 0.5 or 0.6, is attributed to the initial reaction of the primary amine, later supplemented by the secondary amine. In isothermal curing, E_α continues to decrease even beyond $\alpha = 0.8$, whereas in nonisothermal curing the value of E_α increases for degrees of conversion greater than about 0.7. This last is because of etherification, either via the secondary amine or catalyzed by the onium ion (Fig. 9), which takes place predominantly during the later stages of cure, and has a higher activation energy than for the reaction of the epoxy with the primary and/or secondary amines.[37] This behavior is in agreement with the observations of Zvetkov on the nonisothermal cure of DGEBA with *m*-phenylene diamine.[38] In Figure 6, the nanocomposites with MMT contents of 5% and more show a smaller increase in E_α toward the end of the reaction due to the catalytic effect of the onium ion. However, the sample with only 2% MMT content shows a greater increase in E_α, for reasons that are not clear.

Regarding the effect of clay content on the activation energy, the assertion of Becker et al.[9] that E generally decreases as the clay concentration increases is not really supported either by the present results (see Table IV) or, in general, by other literature data,[12,16,39] where any decrease is small and not convincing. Although the modified clay acts as a catalyst for the cure reaction, seen for example in the advance of the cure in both isothermal and nonisothermal conditions (Figs. 2 and 3, respectively), which would be consistent with a reduction in activation energy as the clay content increased, it is not at all evident that an average or other unique value of the activation energy for the whole reaction would follow this simple reasoning. In particular,

the Kissinger method, which has been applied here and in reference 12, uses the data corresponding to the peak heat flow, and hence essentially determines the activation energy for the early stages of the reaction in which the primary amine dominates. More generally, the complexity of the overall reaction, which includes the reactions of the epoxy with both primary and secondary amines as well as the etherification reactions, would introduce the different activation energies for these various reactions, not all of which would necessarily have the same dependence on the clay content.

Kinetic analysis

The curing reaction of the resin without clay, sample EPJ, closely follows eq. (9) in that the data are well described by a single straight line in a plot of ln [ϕ e^x] versus ln [$\alpha^{m/n}$ $(1 - \alpha)$]. In contrast, it has been seen that the curing reaction for the nanocomposites does not follow this theoretical relationship. Instead, there is a separation into two rather well-defined regions characterized by different slopes, this effect being particularly marked in nonisothermal cure (Fig. 8). The value of α at the crossover point from the first region to the second region can be established by means of the degree of conversion curve, which indicates that $\alpha \approx 0.68$ at this point for NEPAJ10. In fact it transpires that for nonisothermal cure the crossover point occurs at about this value of α for all the nanocomposite systems. Interestingly, this is also approximately the value of α for which the activation energy obtained from nonisothermal cure begins to show an upturn in Figure 6, attributed to the influence of the homopolymerization reaction.

The inability of the autocatalytic model to describe correctly the experimental data for the nanocomposites over the whole range of conversion is also demonstrated by the appearance of the $y(\alpha)$ and $z(\alpha)$ functions, again particularly for the nonisothermal cure as shown in Figure 7. Although these functions display, to a reasonable approximation, unique curves for the whole range of values of isothermal cure temperature and heating rate, respectively, as is required by the theory,[18] there are some deviations, particularly toward the end of the reaction. In fact it is the usual case that such deviations, generally small but occasionally much more marked, are observed in practice. What is particularly evident in Figure 7 is that the MMT content plays an important role: for the sample without MMT [EPJ, Fig. 7(a)] the superposition of the data for all the experiments is significantly better than for the sample with 10 wt % MMT [NEPAJ10, Fig. 7(b)]. The appearance of Figure 7(b) is typical for these curves of $y(\alpha)$ and $z(\alpha)$, where the nonisothermal cure of the nanocomposites is characterized by a distinct spreading of the $y(\alpha)$ curves for different heating rates, and particularly so in the region of low degrees of conversion (α less than 0.3, approximately).

There is no trend of a systematic variation of either m or n with either temperature in the isothermal cure (overlooking a possibly rogue value for NEPAJ20 at 100°C) or with heating rate in the nonisothermal cure, which is what would be expected theoretically. Nor is there any systematic variation of these two exponents with MMT content, the overall average values being approximately $m = 0.14$ and $n = 1.7$ for the isothermal cure, and $m = 0.32$ and $n = 2.2$ for the nonisothermal cure. Both of these results are consistent with the usual observation that the sum of m and n should be approximately 2, even though the increase of both m and n on going from isothermal to nonisothermal cure is unexpected. The significant difference between the values of m and n for the isothermal and nonisothermal cures implies a different kinetics in the two cases, and it seems that the isothermal cure is less autocatalytic, indeed closely resembling a reaction of order n in view of the small value for m.

The relative uniformity of the parameter values for the nonisothermal cure at different heating rates, at least during the first stage of the two-stage reaction, would suggest that it should be possible to model rather well this initial part of the nonisothermal reaction over the whole range of heating rates, which is indeed the case. Figure 10 shows the fit of the autocatalytic model (dashed lines) to the nonisothermal cure data (points) for the sample NEPAJ10 using the parameter values listed in Table VI. It can be seen that the initial parts of these curves are fit very well, but that a consistent deviation occurs at temperatures just beyond the peak. This deviation appears as a shoulder on the high temperature side of these bell-shaped curves, making them rather

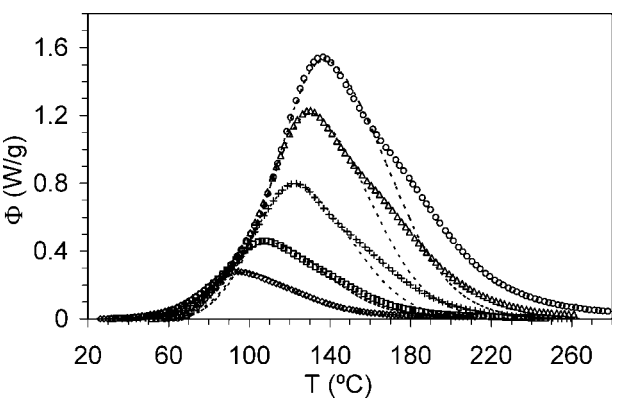

Figure 10 Fit of the autocatalytic model (dashed lines) to the nonisothermal data (points) obtained for NEPAJ10 at heating rates of 2.5, 5, 10, 15, and 20 K/min (in order, from bottom to top).

asymmetric, and suggesting the additional contribution of a different reaction. Similar asymmetric heat flow curves, with a shoulder on the high temperature flank, can be seen in other work on the cure of epoxy-MMT systems[9,12,40] while the appearance of two separate peaks, the one at higher temperature being attributed to the presence of the organically modified MMT, has also been reported.[41]

The appearance of this shoulder occurs at values of α of approximately 0.6 to 0.7, which is the same range of α in which the change of slope is observed in plots such as that in Figure 8. It represents an increase in the rate of cure in comparison with that predicted by the autocatalytic model based upon a single reaction mechanism, which would be consistent with the introduction of an extra reaction mechanism, namely that of homopolymerization catalyzed by the onium ion. Although there is no shoulder visible in the isothermal cure curves, such as those shown in Figure 2, the relevant double logarithmic plots indicate that there is indeed a change in the predominant reaction mechanism, even if the change in slope is not as marked as it is for nonisothermal cure.

Effect of MMT content

One of the principal objectives of this work is to determine the procedures for the fabrication of epoxy-nanoclay nanocomposites with enhanced properties. Of major importance in this respect is the effect of the nanoclay content. In the isothermal cure process, for any given isothermal cure temperature there is a trend of a reduction in the T_g of the partially cured sample as the MMT content increases, this reduction still being evident even in the fully cured samples after a second scan (see $T_{g,\text{part}}$ and $T_{g,f,\text{iso}}$ in Table II). The advance of the cure reaction on the addition of MMT, noted earlier, clearly has an influence on the final network structure. Concurrently, increasing MMT content also leads in general to a reduction in the total heat of cure at any temperature (Table II). These results are consistent with the catalysis of a homopolymerization reaction by the onium ion of the modified MMT: in the first place, this would result in an excess of diamine in the epoxy-diamine crosslinking reaction, off-stoichiometric reactions commonly leading to reduced T_g values[42]; and, in the second place, the heat of reaction for homopolymerization is smaller than that for the epoxy-diamine reaction.[43,44]

The reduction in the heat of reaction with increasing MMT content is even more clearly evident in the nonisothermal cure data (Table III), which are plotted in Figure 11. Here it can be seen that, on the addition of MMT, the heat of reaction in general decreases from that found for the epoxy-amine reaction in the absence of clay, which falls within the range 104 to 108 kJ/ee,

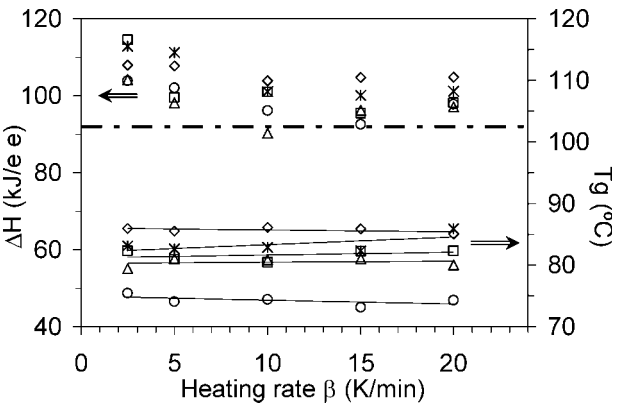

Figure 11 Dependence of the heat of reaction, ΔH_{tot}, and of the glass transition temperature, T_g, on the heating rate in nonisothermal cure for the five systems studied: EPJ (◇), NEPAJ2 (∗), NEPAJ5 (□), NEPAJ10 (△) and NEPAJ20 (○). The dash-dotted line indicates the heat of reaction for etherification. For the T_g data, the lines are linear least squares fits.

approximately, though slightly larger values are seen for NEPAJ2 at 2.5 and 5 K/min and for NEPAJ5 at 2.5 K/min. There is also a trend of decreasing heat of reaction as the heating rate increases for any given clay content, approaching values equal to that found for the etherification reaction,[43,44] indicated by the dash-dotted line at 92 kJ/mol. This is consistent with the observations from Figure 10, for example, where the departure of the experimental heat flow data from the theoretical autocatalytic curves, attributed to the etherification reaction, is hardly noticeable for heating rates of 2.5 and 5 K/min, but is much more significant for the faster heating rates. In contrast, Figure 11 also shows that, while the T_g of the fully cured system decreases rather systematically with increasing clay content, it is essentially independent of the heating rate for all the clay contents studied.

Nanostructure development

Support for the observations discussed earlier can be obtained when we compare the SAXS patterns for samples cured dynamically at 15 and 5 K/min, as shown in Figure 12(a,b), respectively, for sample NEPAJ10. It can be seen that for both cure schedules there is a very strong central scattering, corresponding to *d*-spacings greater than about 8 nm, implying in both cases at least the likelihood of considerable exfoliation, but the important distinction between them is that the faster cure rate [Fig. 12(a)] shows intense scattering corresponding to a *d*-spacing of 1.41 nm, whereas the slower cure rate [Fig. 12(b)] shows no sign of any such ordering. For a dynamic cure rate of 2.5 K/min, a pattern very similar to that for the 5 K/min rate was observed, with no sharp rings being seen for the (001) planes, while the pattern for a cure

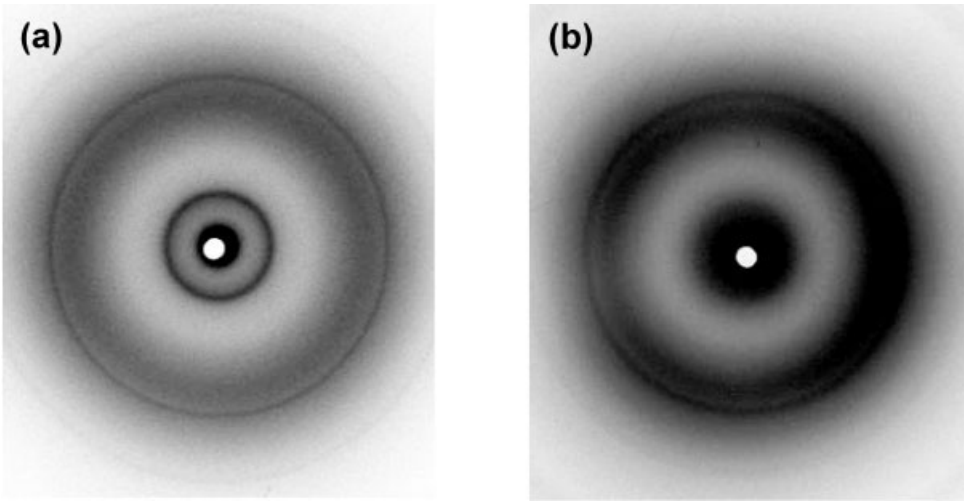

Figure 12 Small angle X-ray scattering patterns for samples of NEPAJ10 cured dynamically at heating rates of (a) 15 K/min and (b) 5 K/min.

rate of 20 K/min was very similar to that for 15 K/min, with intense scattering at a spacing of 1.42 nm.[45]

The question of why a fast curing rate should result in a *d*-spacing of 1.4 nm, smaller than that of the intercalated resin/clay mixtures (typically about 3.7 nm) and smaller even than that of the clay alone (2.1 nm), is interesting. It is speculated here that this might be attributed to the presence of clay agglomerations in the resin/clay mixture, the existence of which was noted earlier, in the discussion about the quality of dispersion. Although the resin intercalates into the clay galleries independently of how well or badly the clay is dispersed in the resin, as indicated by SAXS of the resin/clay mixtures, the significant amount of exfoliation (as identified by the intense scattering at large spacings seen in Fig. 12) that occurs when the curing agent is added and the cure reaction proceeds is believed to take place principally in those clay tactoids that are well dispersed and for which access to the diamine is relatively easy. In contrast, the highly agglomerated regions do not have the same access to the diamine, and at the same time are increasingly restricted by the growth of the network around them, which, among other things, results in a shrinkage on cure, and consequently compresses the clay layers in the agglomerated regions. At the same time, the lack of access of diamine to these regions favors instead the homopolymerization reaction catalyzed by the onium ion, leading to the reduction in the heat of reaction noted above and to the separation of the cure kinetics into two distinct regions, manifest in particular as a shoulder in the dynamic cure curves at the faster heating rates. In this respect, therefore, the dispersion of the clay in the resin before the addition of the curing agent would be of great importance in the reaction kinetics and in the nanostructure development, and is the subject of our continuing research.

Similar, but subtly distinct, results are observed for the isothermal cure of nanocomposites containing 10 wt % clay, as exemplified by the SAXS pattern in Figure 13 for the isothermal cure of NEPAJ10 at 100°C. Here, an intense scattering can be seen corresponding to *d*-spacings larger than about 8 nm, representing a significant amount of exfoliation, together with a strong ring at 1.80 nm, again much less than the *d*-spacing for both the intercalated resin/clay mixtures and the modified clay alone. The same pattern is found for isothermal cure at

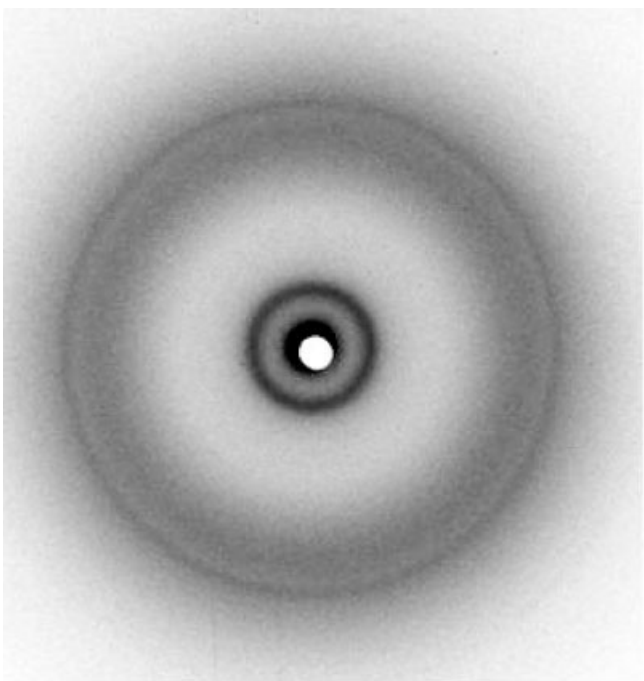

Figure 13 Small angle X-ray scattering pattern for sample of NEPAJ10 cured isothermally at 100°C.

70°C,[45] but with a smaller contribution from the exfoliated clay and with the strong ring at 1.82 nm. The presence of diffraction corresponding to *d*-spacings of the order of 1.8 nm in these isothermally cured samples is again considered to indicate that significant agglomerations remained in the resin/clay mixture prior to the addition of the diamine, and that the combination of the cure of the surrounding network and homopolymerization within these agglomerations leads to a reduction in the *d*-spacing of the intercalated clay in these regions.

In fact, very similar diffraction patterns are obtained from resin/clay mixtures even without the addition of the curing agent, if the mixtures are preconditioned for long times at room temperature. Such preconditioning has been shown to have an important effect on the exfoliation process,[6] and has been interpreted in terms of a homopolymerization reaction catalyzed by the onium ion of the organically modified clay.[17] A good illustration of this is provided by the SAXS pattern in Figure 14, obtained for a mixture of resin with 10 wt % MMT which had been preconditioned at room temperature for 18 months, where a very significant amount of scattering corresponding to distances greater than about 8 nm can be seen, together with strong diffraction at a *d*-spacing of 1.96 nm. When homopolymerization takes place at much higher temperatures during thermogravimetric analysis over a temperature range from ambient to 600°C, the degraded product is observed to have the consistency of a highly expanded powder, as was first noted by Lan et al.,[36]

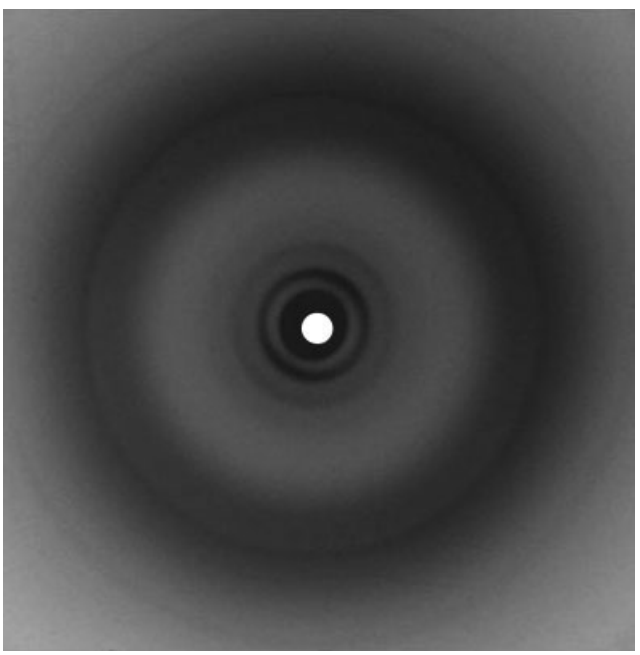

Figure 14 Small angle X-ray scattering pattern for mixture of Epon 828 with 10 wt % MMT, preconditioned at room temperature for 18 months.

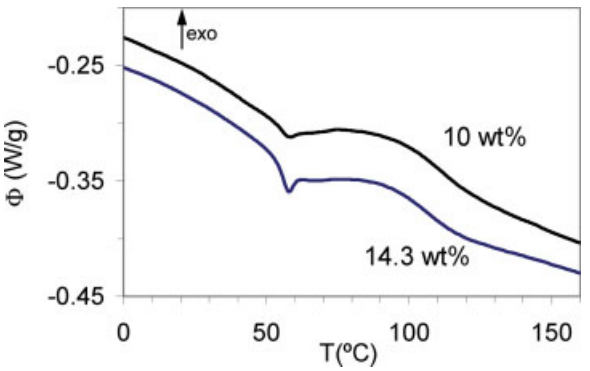

Figure 15 DSC scans at 10 K/min on preconditioned resin/clay mixtures with 10 wt % and 14.3 wt % MMT, as shown, immediately after complete homopolymerization by heating to 280°C, showing the existence of two glass transition regions. Note that only a part of the complete scan from −70°C is shown here. [Color figure can be viewed in the online issue, which is available at www.interscience.wiley.com.]

implying extensive exfoliation of the clay layers. The intense scattering at the center of the SAXS pattern of Figure 14 suggests that a significant amount of exfoliation is taking place, even at room temperature, by the same process of homopolymerization.

In a further experiment, when this same 10 wt % MMT mixture, preconditioned for a slightly longer time at room temperature (19.5 months), is heated in the DSC at 10 K/min from ambient temperature to 280°C to promote the complete homopolymerization of the sample, the heat of reaction is measured as 457 J/g of epoxy, considerably less than the 611 J/g found for the Epon 828 alone, confirming that a significant amount of reaction had already occurred at room temperature because of homopolymerization. A second DSC scan from −70°C to 160°C at 10 K/min, immediately following the complete homopolymerization, is shown in Figure 15, where two glass transitions can be seen: the first occurs at about 50°C, with an endothermic peak close to 60°C, much higher than the peak endotherm temperature of about −10°C in the epoxy resin alone,[17] while the second glass transition is broader and centered at about 110°C. Similar results are also shown in Figure 15 for a mixture of resin with 14.3 wt % MMT, preconditioned at room temperature for 20 months, with the greater MMT content in this mixture now inducing a larger endothermic peak at the lower glass transition. These DSC results indicate the existence of two regions in which the epoxy has different molecular mobilities, in support of the nanostructural development proposed earlier.

CONCLUSIONS

In the present work, we have studied the kinetics of the cure reaction of nanocomposites based on epoxy

resin with organically modified montmorillonite clay and cured with a nominally stoichiometric ratio of a diamine crosslinking agent. The reactions have been monitored by differential scanning calorimetry in both isothermal and dynamic modes, and the kinetics have been analyzed by Málek's method. In both isothermal and nonisothermal cure, the effect of the addition of MMT is to advance the reaction as a result of the catalytic action of the organically modified clay. With respect to the kinetic analysis, although the autocatalytic (Sesták-Berggren) model is shown to be the more appropriate to use for this reaction, it is found that it is not possible to describe the complete reaction, particularly in the nonisothermal mode, with this simple model. The complexity of the reaction is particularly evident from the double logarithmic plot which should give the exponent n of the autocatalytic equation from the slope; this plot clearly shows two straight line regions, which can be associated with two separate stages in the reaction. This can also be seen in the heat flow curve during the reaction, again especially in nonisothermal mode, which shows a pronounced shoulder on the high temperature flank of the bell-shaped curve, beginning at degrees of cure of about 0.6. For degrees of cure higher than about this value, there is also a marked change in the trend of the isoconversional activation energy as a function of the degree of cure, again suggestive of a change of reaction mechanism. These effects are interpreted in terms of an etherification reaction taking place in the nanocomposite, catalyzed by the onium ion of the organically modified clay. One consequence of this is that epoxy groups are consumed without reaction with the diamine crosslinking agent, thus leaving an excess of unreacted amine. The effect of this is to cause the epoxy-diamine reaction to be off stoichiometric, with a resulting reduction in the glass transition of the cured nanocomposite, a reduction that is greater the larger is the MMT content. Simultaneously, the heat of reaction also decreases with increasing MMT content, attributed to the smaller heat of reaction of the etherification reaction.

The effect of different cure schedules on the nanostructure has also been investigated by small angle X-ray scattering on the cured samples. In nonisothermal cure, an exfoliated nanostructure is obtained when the heating rate is slow (2.5 and 5 K/min), as evidenced by the absence of the (001) spacings observed in the intercalated resin/clay mixtures and by strong scattering at distances larger than about 8 nm, whereas for faster heating rates (15 and 20 K/min), as well as for isothermal cure at 70°C and 100°C, the exfoliation is accompanied by the occurrence of sharp d-spacings of the order of 1.4 nm and 1.8 nm for isothermal and nonisothermal cure, respectively. The appearance of such d-spacings, at distances smaller than the d-spacing for the modified clay before intercalation of the resin, is attributed to the presence of clay agglomerations in the original mixture, to which access of the diamine is restricted and hence for which homopolymerization is favored. The reduction in d-spacing is caused by the volumetric shrinkage which takes place during the curing reaction and network formation occurring in the regions surrounding these agglomerations. Similar d-spacings are observed also in resin/clay mixtures, without the addition of any crosslinking agent, which are stored (preconditioned) for long periods at room temperature, during which a homopolymerization process takes place. It is concluded from these results that, although the quality of the initial dispersion of the clay in the resin has no effect on the intercalation process, it does have an important influence on the nanostructure development during cure, and this is therefore the subject of continuing work.

The authors are grateful to J. Málek and P. Pustkova for the provision of the TAS software for the analysis of the kinetic data, and to Menno Schoenfeld of Nordmann-Rassmann GmbH for the provision of the modified clays. J.M.H. is grateful for a Ramón y Cajal research contract.

References

1. Alexandre, M.; Dubois, P. Mater Sci Eng 2000, 28, 1.
2. Ray, S. S.; Okamoto, M. Prog Polym Sci 2003, 28, 1539.
3. Becker, O.; Simon, G. P. Adv Polym Sci 2005, 179, 29.
4. Lan, T.; Kaviratna, P. D.; Pinnavaia, T. J Chem Mater 1995, 7, 2144.
5. Kornmann, X.; Lindberg, H.; Berglund, L. A. Polymer 2001, 42, 4493.
6. Benson Tolle, T.; Anderson, D. P. J Appl Polym Sci 2004, 91, 89.
7. Butzloff, P.; D'Souza, N. A.; Golden, T. D.; Garrett D. Polymer Eng Sci 2001, 41, 1794.
8. Shi, Z.; Yu, D. S.; Wang, Y.; Xu, R. Eur Polym J 2002, 38, 727.
9. Becker, O.; Simon, G. P.; Varley, R. J.; Halley, P. J. Polymer Eng Sci 2003, 43, 850.
10. Shi, Z.; Yu, D. S.; Wang, Y.; Xu, R. J Appl Polym Sci 2003, 88, 194.
11. Chen, D. Z.; He, P. S. Comp Sci Technol 2004, 64, 2501.
12. Ton-That, M. T.; Ngo, T. D.; Ding, P.; Fang, G.; Cole, K. C.; Hoa, S. V. Polymer Eng Sci 2004, 44, 1132.
13. Mohan, T. P.; Ramesh Kumar, M.; Velmurugan, R. Polym Int 2005, 54, 1653.
14. Shen, M. M.; Lu, M. G.; Chen, Y. L.; Ha, C. Y. J Appl Polym Sci 2005, 96, 1329.
15. Yei, D. R.; Fu, H. K.; Chen, W. Y.; Chang, F. C. J Polym Sci Part B: Polym Phys 2006, 44, 347.
16. Ivankovic, M.; Brnardic, I.; Ivankovic, H.; Mencer, H. J. J Appl Polym Sci 2006, 99, 550.
17. Hutchinson, J. M.; Montserrat, S.; Román, F.; Cortés, P.; Campos, L. J Appl Polym Sci 2006, 102, 3751.
18. Málek, J. Thermochim Acta 1992, 200, 257.
19. Friedman, H. L. J Polym Sci C: Polym Symp 1964, 6, 183.
20. Málek, J.; Mitsuhashi, T.; Criado, J. M. J Mater Res 2001, 16, 1862.

21. Kissinger, H. E. Anal Chem 1957, 29, 1702.
22. Ozawa, T. J Therm Anal 1970, 2, 301.
23. Málek, J. Thermochim Acta 2000, 355, 239.
24. Montserrat, S.; Málek, J. Thermochim Acta 1993, 228, 47.
25. Ratna, D.; Manoj, N. R.; Varley, R.; Singh Raman, R. K.; Simon, G. P. Polym Int 2003, 52, 1403.
26. Chin, I. J.; Thurn-Albrecht, T.; Kim, H. C.; Russell, T. P.; Wang, J. Polymer 2001, 42, 5947.
27. Benson Tolle, T.; Anderson, D. P. Comp Sci Technol 2002, 62, 1033.
28. Becker, O.; Varley, R. J.; Simon, G. P. Polymer 2002, 43, 4365.
29. Ratna, D.; Becker, O.; Krishnamurthy, R.; Simon, G. P.; Varley, R. J. Polymer 2003, 44, 7449.
30. Becker, O.; Varley, R. J.; Simon, G. P. Eur Polym J 2004, 40, 187.
31. Liu, W.; Hoa, S. V.; Pugh, M. Polym Eng Sci 2004, 44, 1178.
32. Tanaka, Y.; Bauer, R. S. In Epoxy Resins: Chemistry and Technology, 2nd ed.; May, C. A., Ed.; Marcel Dekker: New York, 1988; Chapter 3, p 285.
33. Pascault, J.-P.; Sautereau, H.; Verdu, J.; Williams, R. J. J. Thermosetting Polymers; Marcel Dekker: New York, 2002; Chapter 2.
34. Cole, K. C. Macromolecules 1991, 24, 3093.
35. Wang, M. S.; Pinnavaia, T. J. Chem Mater 1994, 6, 468.
36. Lan, T.; Kaviratna, P. D.; Pinnavaia, T. J. J Phys Chem Sol 1996, 57, 1005.
37. Cole, K. C.; Hechler, J. J.; Noël, D. Macromolecules 1991, 24, 3098.
38. Zvetkov, V. L. Polymer 2001, 42, 6687.
39. Xu, W.; Bao, S.; Shen, S.; Wang, W.; Hang, G.; He, P. J Polym Sci Part B: Polym Phys 2003, 41, 378.
40. Xu, W.-B.; Bao, S.-P.; Shen, S.-J.; Hang, G.-P.; He, P.-S. J Appl Polym Sci 2003, 88, 2932.
41. Nigam, V.; Setua, D. K.; Mathur, G. N.; Kar, K. K. J Appl Polym Sci 2004, 93, 2201.
42. Morgan, R. J.; Kong, F.-M.; Walkup, C. M. Polymer 1984, 25, 375.
43. Klute, C. H.; Viehmann, W. J Appl Polym Sci 1961, 5, 86.
44. Dell'Erba, I. E.; Williams, R. J. J. Polymer Eng Sci 2006, 46, 351.
45. Román, F.; Hutchinson, J. M.; Montserrat, S. J Thermal Anal Calorim 2007, 87, 113.